Separate pathways of RNA recruitment lead to the compartmentalization of the zebrafish germ plasm

Elizabeth V. Theusch [1], Kimberly J. Brown [2], Francisco Pelegri *

Laboratory of Genetics, University of Wisconsin–Madison, 425-G Henry Mall, Madison, WI 53706, USA

Abstract

The maternal RNAs *vasa*, *dead end*, *nanos1*, and *daz-like* all become localized to the peripheral ends of the first and second cleavage furrows, where they form part of the zebrafish germ plasm. We show that aggregates of a first class of germ plasm components, which include *dead end*, *nanos1*, and *vasa* RNAs, are initially present in a wide cortical band at the animal pole. Aggregates containing these three RNAs appear to be associated with f-actin, which during the first cell cycle undergoes a microtubule-dependent movement towards the periphery as well as circumferential alignment. These cytoskeletal rearrangements lead to the further aggregation of particles containing these RNAs and their concomitant recruitment to the forming furrow. Aggregates containing a second class of germ plasm RNA components, which include the transcript for *daz-like*, translocate along the plane of the cortex towards the animal pole, where they are recruited to the germ plasm. After recruitment to the furrow, these two classes of RNAs occupy overlapping yet distinct regions of the germ plasm, and this arrangement is maintained during the early cleavage stages. Our observations suggest that separate pathways of RNA recruitment facilitate the compartmentalization of the zebrafish germ plasm.
© 2005 Elsevier Inc. All rights reserved.

Introduction

In many animals, including *Caenorhabditis elegans*, *Drosophila*, *Xenopus*, and the zebrafish, the specification of the germ line is a cell fate decision that depends upon the asymmetric localization of a specialized cytoplasm termed the germ plasm (reviewed in Wylie, 1999). This germ plasm is an electron-dense structure containing a collection of maternal RNAs and proteins that were originally deposited in the oocyte and are eventually segregated to the primordial germ cells.

In the zebrafish, ultrastructurally defined germ plasm forms at the furrows of the first and second cleavage divisions (Knaut et al., 2000). Removal of the cytoplasm from these regions results in defects in germ cell determination (Hashimoto et al.,

2004), suggesting that factors in the germ plasm are essential for this process. Several RNAs have been proposed to form part of the zebrafish germ plasm. Zebrafish maternal *vasa* (*vas*) RNA is localized to the cortex of oocytes and, upon activation, concentrates at the base of the blastodisc, between the yolk and cytoplasm, in one-cell embryos (Braat et al., 1999; Howley and Ho, 2000). *vas* RNA subsequently becomes enriched at the distal ends of the cleavage furrows in 2-cell and 4-cell embryos, first as rod-like structures and subsequently as compact aggregates at the periphery of the furrow (Yoon et al., 1997; Pelegri et al., 1999, reviewed in Pelegri, 2003). These aggregates subsequently ingress into four cells at the 32-cell stage and segregate asymmetrically during cell division until the sphere stage (Braat et al., 1999; Knaut et al., 2000). The maternal RNA for the zebrafish genes *dead end (dnd)* and *nanos1 (nos1)* were also found to be enriched at the distal ends of the cleavage furrows in 2-cell and 4-cell embryos (Weidinger et al., 2003; Köprunner et al., 2001). More recently, maternal RNAs for *daz-like (dazl)* and *bruno-like*, which are located at the vegetal pole during oogenesis and in the freshly laid egg,

have also been found localized to the ends of the cleavage planes of 4-cell stage embryos (Maegawa et al., 1999; Hashimoto et al., 2004).

During development, microtubules and actin microfilaments work in concert to move many cellular components, including RNAs (reviewed in Kloc and Etkin, 2005). We have previously shown a role for a microtubule network at the furrow, the furrow microtubule array (FMA), in the peripheral movement and aggregation of the *vas* RNA during the late stages of furrow maturation (Pelegri et al., 1999). However, the cytoskeletal requirements for other aspects of the early segregation of germ plasm RNA components, such as their recruitment to the forming furrow, have not been studied in detail. The *vas* RNA is associated with the actin cortex in oocytes and early embryos (Knaut et al., 2000), and f-actin, like the germ plasm RNAs, is recruited to the forming furrow (Kishimoto et al., 2004; A. Menzie and F.P., unpublished). Thus, it seems likely that the actin-based cytoskeleton also plays a role in the early segregation of the *vas* RNA and other germ plasm components. However, a direct role for the cytoskeleton in germ plasm recruitment at the furrow has been difficult to test, since formation of the furrow itself is inhibited when the function of the cytoskeleton is compromised (Pelegri et al., 1999; Knaut et al., 2000).

In this report, we examine in detail the expression patterns of *vas*, *dnd*, *nos1*, and *dazl* maternal RNAs during egg activation and the early cleavages and describe separate pathways of segregation which eventually converge into the recruitment of the germ plasm aggregate at the maturing furrow. We find that for three of these RNAs, *vas*, *dnd*, and *nos1*, an enrichment of RNA-containing aggregates already exists at the base of the blastodisc in the freshly laid egg. Moreover, these RNAs are associated with a filament network that appears to be composed of f-actin bundles. During the first cell cycle, both RNA aggregates and f-actin move towards the periphery of the embryo in a process that appears to be dependent on astral microtubules. This cytoskeletal reorganization leads to the formation of larger aggregates, and the concomitant lateral transport of these aggregates results in recruitment of RNA at the furrow. A fourth RNA, for the *dazl* gene, is recruited to the germ plasm through a separate pathway involving the translocation of RNA aggregates along the egg cortex. Our data suggest that this dual mechanism of segregation has evolved to facilitate the formation of a compartmentalized germ plasm.

Results

Different sets of germ plasm RNAs reach the furrow through separate segregation pathways

We investigated the expression patterns of RNAs for the *dnd*, *nos1*, *vas*, and *dazl* genes using in situ hybridization and detection with fluorescent substrates, which allowed observations of RNA-containing aggregates at a high resolution. Parallel analysis using the standard light-visible blue substrate provided similar overall patterns but with a reduced resolution

(data not shown). Embryos were fixed and analyzed with fluorescent in situ hybridization (FISH) every 5 min during the first 50 min after fertilization, and a selection of stages is presented in Fig. 1. RNAs for the genes *vas*, *dnd*, and *nos1* can be detected at the animal pole in cortical aggregates within a wide band at the periphery of the blastodisc but not in the region closest to the animal pole (Figs. 1A–C). An RNA-free region at the animal pole is already observed in eggs collected immediately after egg activation (3 min post-fertilization (p.f.); data not shown), suggesting that the region containing RNA aggregates is already prepatterned in the mature oocyte.

On the other hand, *dazl* RNA aggregates cannot be detected near the animal pole in early embryos (Figs. 1D, H), even though *dazl* RNA aggregates can be clearly detected at the vegetal pole during these stages (data not shown, see also Fig. 6). *dazl* RNA-containing aggregates begin to be detected in the animal pole regions at about 45 min p.f. (Fig. 1L), approximately the same time at which the RNA accumulates at the forming furrow (arrow in Fig. 1L). Thus, although all four RNAs are recruited to the forming furrow, RNAs for *dnd*, *nos1*, and *vas* are already present in the animal pole in the freshly laid egg, while *dazl* RNA arrives to the animal pole from the vegetal region at a later stage. Based on their different times of appearance at the animal region, we refer to the *dnd*, *nos1*, and *vas* RNAs as the early animal germ plasm RNAs, while *dazl* is also referred to as a vegetally localized germ plasm RNA.

Prepattern, fibrillar localization, and furrow recruitment of early germ plasm RNA-containing aggregates

As the first furrow forms, the aggregates of early animal germ plasm RNAs are recruited as a rod-shaped structure at the peripheral region of the furrow (Figs. 1E–G, see also Figs. 2I–K). As the furrows begin to form, the limits of this rod-like domain along the length of the furrow are similar to the boundaries of the band-like region containing more dispersed RNA aggregates (Figs. 1E–G, I–K, see also Figs. 2I–K). This suggests that RNA aggregates undergo recruitment at the furrow by lateral transport towards the furrow from the immediately adjacent region. This interpretation is also supported by the appearance of aggregate-free zones on both sides of the furrow (brackets in Fig. 2K) in the zone immediately adjacent to the recruited germ plasm (arrows in Figs. 2J, K).

As development proceeds, the internal (closest to the center of the blastodisc) boundaries of the RNA-rich domain appear at progressively more peripheral positions. This results in the progressive narrowing of these domains (solid double-ended arrows in Figs. 2A, E, I) and an increase in the diameter of the central aggregate-free region (dashed double-ended arrows in Figs. 2A, E, I). Thus, the movement towards the periphery of the aggregates closest to the animal pole following egg activation results in the further peripheral localization of the prepatterned field of RNA aggregates.

Strikingly, imaging of fields of the RNA-rich domain at high magnification reveals that aggregates are not arranged randomly within this region but rather tend to be aligned as beads on a
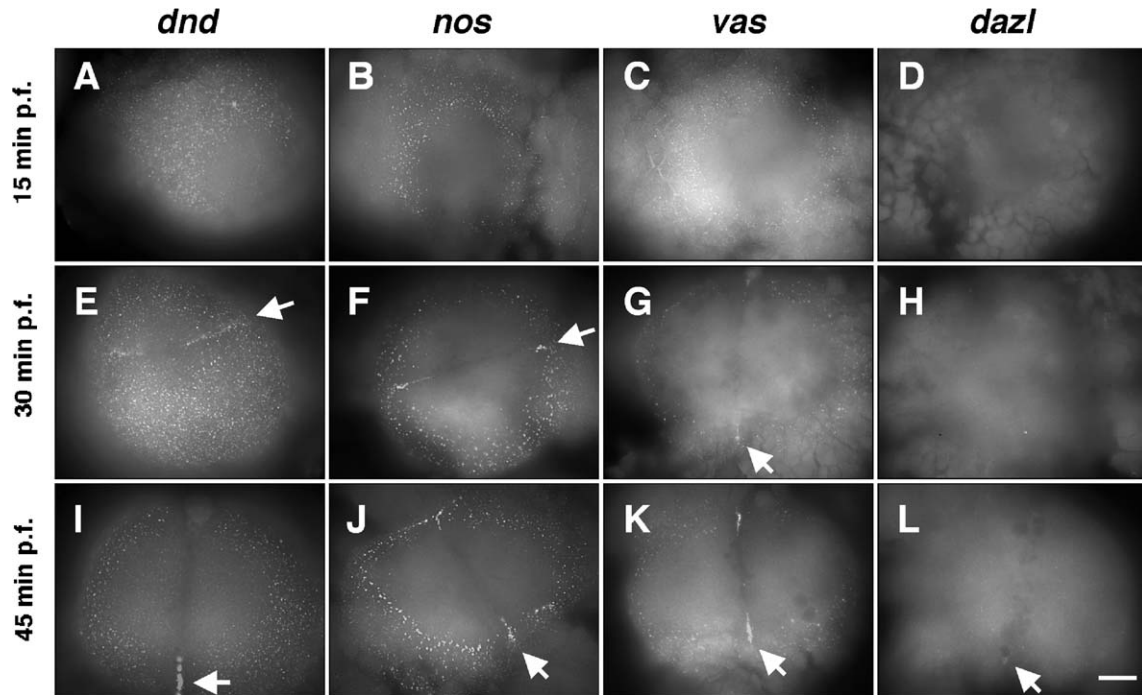
Fig. 1. Endogenous patterns of RNA localization of *dnd*, *nos1*, *vas*, and *dazl* RNAs during the first cell cycle. Animal views of embryos fixed at progressively older stages of development (A–D: 15 min p.f.; E–H: 30 min. p.f.; I–L: 45 min p.f.) and labeled using FISH to detect germ plasm RNAs (*dnd* (A, E, I); *nos1* (B, F, J); *vas* (C, G, K); *dazl* (D, H, L). (A–D) Immediately after fertilization, *dnd*, *nos1*, and *vas* RNA aggregates can be observed as a band at the animal pole, while *dazl* RNA aggregates are not initially present in the animal pole. (E–H) During the initiation of furrow formation, RNA aggregates for *dnd*, *nos1*, and *vas* begin to be recruited as a rod at the forming furrow (arrows in E–G). At this stage, *dazl* RNA is not yet detectable at the furrows (H). (I–L) As the furrow matures, there is an increase in the amount of *dnd*, *nos1*, and *vas* RNAs recruited at the furrow, and *dazl* RNA becomes detectable at the furrow (arrows in I–L). Scale bar in panel (L) represents 100 μm.

string along lines that appear to form a network (Figs. 2C, D, G, H). Initially, lines of aggregates in this network are arranged in an apparent random orientation with respect to the center of the embryo (Figs. 2C, D). However, as embryos develop during the first cell cycle, the lines of aggregates tend to orient themselves circumferentially, as seen on an animal pole view, along the periphery of the blastodisc (Figs. 2G, H). The combined action of the movement towards the periphery of lines of aggregates and their circumferential alignment results in sets of parallel lines of aggregates that highlight the internal boundary of the aggregate-rich region, between the "cleared" central region and the outer region of the domain which has not yet undergone these rearrangements (Figs. 2F, G, arrowheads). Concomitant with these processes, there is an increase in the size of RNA-containing aggregates, particularly in the internal boundary region that contains the circumferentially aligned lines of aggregates. These aggregates often appear to have a modular structure, consistent with the idea that they result from the fusion of adjacent smaller aggregates. As development proceeds, circumferentially arranged lines of medium-sized aggregates at the internal boundary of the RNA-rich region become even more apparent (Figs. 2J, K, arrowheads). These observations support a model in which early animal RNAs are bound to filaments which during the first cell cycle are moved towards the periphery and align with each other. This rearrangement in turn facilitates the fusion of RNA particles, resulting in their aggregation into larger sized particles (see Discussion and Fig. 8A).

Cytoskeletal rearrangements during the first cell cycle correlate with the movement of early animal germ plasm RNAs

The arrangement of early animal RNA aggregates along an apparent underlying filamentous network led us to examine in detail the f-actin- and microtubule-based cytoskeleton in embryos at these stages. In a first set of experiments, embryos were fixed every 5 min after fertilization, labeled to detect f-actin using fluorescent phalloidin, and costained with a DNA dye to better ascertain the stage of the cell cycle (selected stages are shown in Fig. 3, DNA stain is not shown). Labeling of f-actin revealed a striking dynamic rearrangement of the microfilament network. As previously reported, immediately after fertilization (5 min p.f.), f-actin is present as a cortical field of short filaments and punctae that represents residual crypts after cortical granule release (Becker and Hart, 1999; data not shown). Soon afterwards (15 min p.f.), f-actin forms a network of microfilament bundles that initially encompasses the entirety of the blastodisc cortex (Figs. 3A–C). As the first cell cycle progresses (30 min p.f.), filaments in this network begin to occupy more peripheral positions on the blastodisc, leaving a clearing in the center of the embryo, and to align themselves along concentric rings (Figs. 3D–F). By the time the first cellular furrow forms, f-actin bundles have formed concentric rings around the periphery of the embryo (Figs. 3G–I). As development proceeds, the thickness and labeling intensity of the f-actin cables increases (compare for example Figs. 3A–C to G–I), suggesting that the rearrangements are associated with
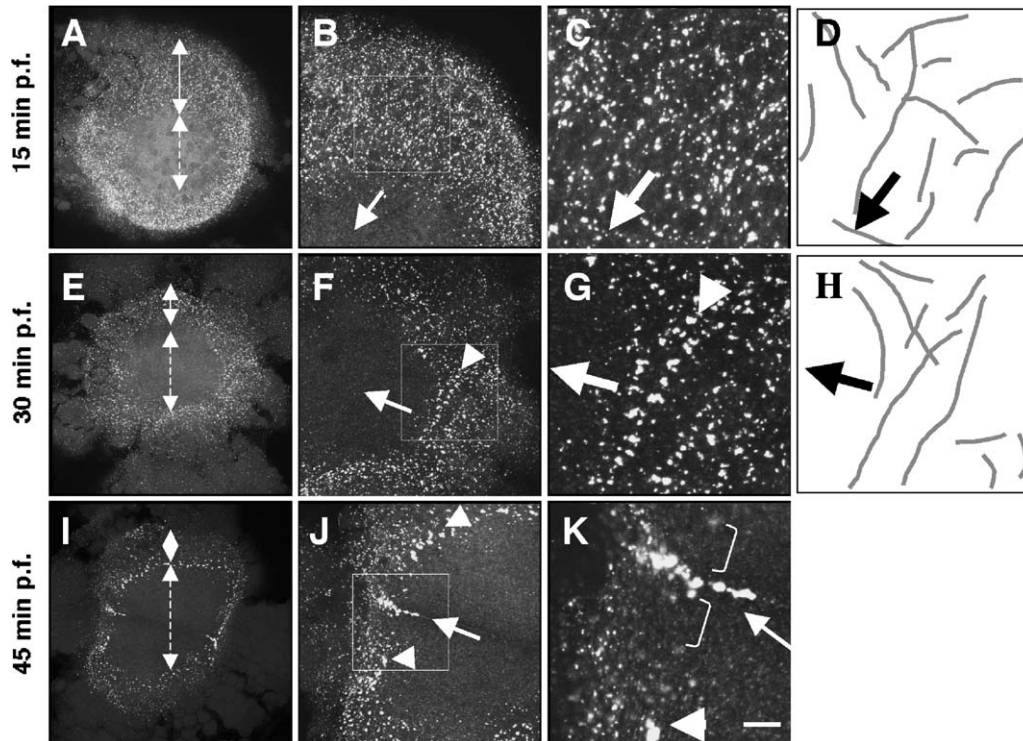
Fig. 2. RNA aggregates lie along a filamentous network, which undergoes movement towards the periphery and circumferential alignment. Animal views of embryos fixed at progressively older stages of development (A–C: 15 min p.f.; E–G: 30 min. p.f.; I–K: 45 min p.f.) and labeled using FISH to detect *nos1* RNA. Panels A–C, E–G, and I–K are progressively higher magnifications of the same embryo (left column: overview; middle and left columns: square in the middle panel is shown in the right panel at a higher magnification). As development proceeds, the diameter of the RNA-free region increases (dashed double ended arrows in A, E, I) and the width of the RNA-rich band decreases (solid double ended arrows in A, E, I), reflecting the movement towards the periphery of RNA aggregates closest to the center of the blastodisc. High magnification views show that RNA aggregates lie along a filamentous network (C, G; traces along a subset of lines of aggregates in these panels are shown in D, H, respectively). The original orientation of the lines of aggregates appears random, but upon development, they tend to align circumferentially (arrowhead in G; arrows in B–D and F–H point to the center of the blastodisc). As these processes occur, the size of the RNA aggregates increases (arrowheads in J, K). Furrow formation accompanies germ plasm recruitment at the furrow (arrows in J, K), which is typically flanked by regions free of RNA aggregates (brackets in K). Scale bar in (K) represents 100 μm (left column), 50 μm (middle column), and 16 μm (right column).

increased bundling of f-actin. The movement towards the periphery and circumferential alignment of the f-actin filaments mimics the behavior of lines of RNA aggregates and suggests that the fibrils along which early animal RNA aggregates are aligned consist of f-actin (see below). This is consistent with previous structural analysis showing that at these stages, germ plasm is associated with the actin cortex (Knaut et al., 2000), and our observations that the number of RNA aggregates at the cortex decreases upon the injection of the f-actin inhibitor latrunculin B (Fig. 5B; 17/19 with reduced number of aggregates within the RNA-rich field in latrunculin-B-injected, compared to 5/20 in control-injected).

We next wanted to address what process may be responsible for the movement towards the periphery and circumferential alignment of the actin network and RNA aggregates. We focused on the analysis of microtubules because of reports that the distal ends of microtubules can mediate the movement of f-actin cables (Sider et al., 1999; Waterman-Storer et al., 2000; Foe et al., 2000), as well as observations of centrally emanating astral microtubules present immediately prior to cell division (Jesuthasan and Strähle, 1997; Jesuthasan, 1998; Pelegri et al., 1999). We therefore fixed embryos every 5 min as above and labeled

them to detect microtubules using an anti-α-tubulin antibody (selected stages are shown in Fig. 4). This analysis shows that between 5 and 20 min p.f. embryos form a monoastral structure which begins to form immediately after fertilization (Figs. 4A, B). This monoastral structure appears to originate from the male pronucleus, as suggested by colabeling of DNA, which allows the identification of the male and female pronuclei by their relationship with the forming second polar body after the resumption of meiosis II induced by egg activation (data not shown). As the first cell cycle proceeds, microtubules in this monoaster lengthen and reach the peripheral edges of the blastodisc, often leaving a region in the center of the embryo with a reduced level of microtubules (Figs. 4C, D). In addition, a local enrichment of microtubules can be observed at the peripheral edges of the blastodisc (inset in Fig. 4D). By 35 min p.f., immediately prior to furrow formation and presumably after centriole replication, the spindle has rearranged into a diastral structure as previously reported (Figs. 4E, F; Jesuthasan and Strähle, 1997; Jesuthasan, 1998; Pelegri et al., 1999). As in the case of the monoastral tubules, tubules of the bipolar asters appear to elongate as the next cell cycle proceeds (Figs. 4G, H) and also appear to show an enrichment at the periphery (arrowhead in
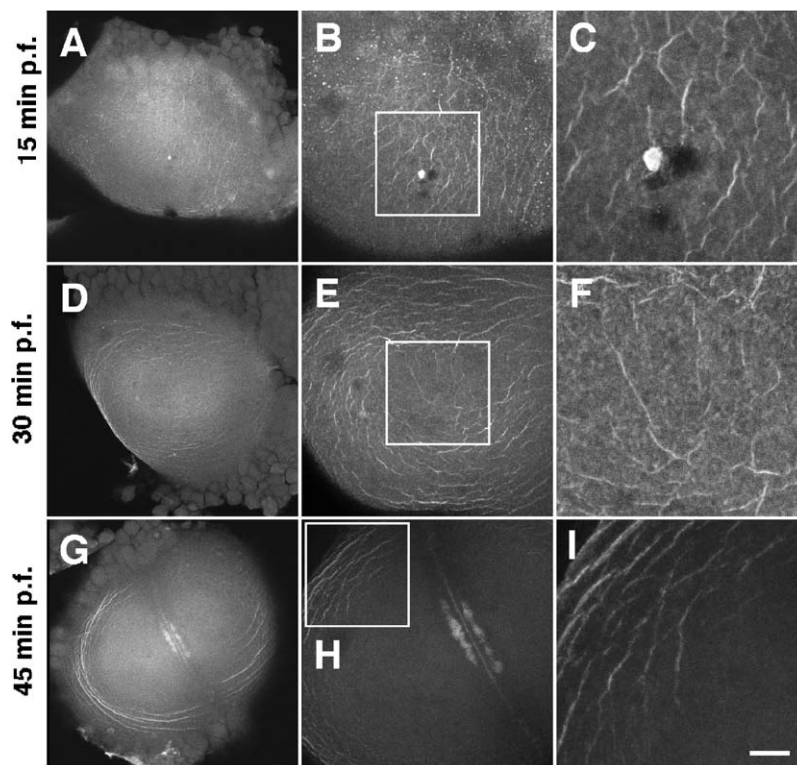
Fig. 3. An f-actin network undergoes arrangements that are similar to those of the RNA-bound filaments. Animal views of embryos fixed at progressively older stages of development (A–C: 15 min p.f.; D–F: 30 min. p.f.; G–I: 45 min p.f.) and labeled with fluorescent phalloidin. Panels A–C, D–F, and G–I are sets of progressively higher magnifications of the same embryo (left column: overview; middle and left columns: square in the middle panel is shown in the right panel at a higher magnification). (A–C) Initially f-actin forms a network of randomly aligned cables. (D–F) As the first cell cycle proceeds, f-actin begins to move towards the periphery (note clearing of f-actin in the center of the blastodisc) and circumferential alignment (note alignment of outer cables). (G–I) These effects become more pronounced at later stages of development. The accumulation of f-actin in panels B, C highlights the second polar body, which forms after egg activation (Dekens et al., 2003). The accumulation of f-actin at the center of the blastodisc in panels G, H corresponds to f-actin enrichments that typically occur at the site of furrow formation (Kishimoto et al., 2004; A. Menzie and F.P., unpublished). Scale bar in panel I represents 100 μm (left column), 50 μm (middle column), and 16 μm (right column).

Fig. 4G). Thus, microtubule asters are present in the embryo at the right time and place to have an effect on the overlying actin network. Specifically, our observations are consistent with the hypothesis that elongating astral microtubules bound to the actin network at their outer ends mediate the movement towards the periphery and reorientation of f-actin bundles.

Changes in microtubule dynamics affect the segregation and recruitment of early animal germ plasm RNAs and the rearrangement of the actin network

In order to test the hypothesis that microtubules are involved in the movement towards the periphery and circumferential alignment of f-actin and RNA aggregates, we tested whether drugs that induce changes in microtubule dynamics lead to predictable changes in these processes. Early embryos were exposed to cell permeable drugs that affect microtubule dynamics at a time after fertilization when the transient enrichment of RNA at the base of the blastodisc has not fully developed (15 min p.f.). After fixation, early animal germ plasm RNA aggregates were labeled using FISH (Figs. 5A–D; for all results in this section, experiments using the standard blue substrate led to similar results, not shown). In addition, similarly treated embryos were labeled to detect f-actin and microtubules using fluorescently labeled phalloidin (Figs. 5E–H) and anti-α-tubulin (not shown), respectively.

Exposure to the microtubule-destabilizing drug nocodazole during the first cell cycle results in the expected reduction in microtubule-based structures and interferes with furrow formation at later stages (data not shown; Pelegri et al., 1999). Nocodazole-treated embryos exhibit changes in the distribution of early germ plasm RNAs at the base of the blastodisc at the one cell stage as detected using FISH analysis. Specifically, nocodazole-treated embryos show a reduction in the peripheral movement of RNA aggregates, resulting in a smaller RNA-free zone in the middle of the embryo (Fig. 5C; 13/19 with reduced central clearing, compared to 3/19 in control-treated embryos). In addition, RNA particles in nocodazole-treated embryos do not form circumferential lines of larger aggregates, consistent with a defect in their aggregation into larger particles. Similarly, labeling with fluorescent phalloidin shows that nocodazole treatment leads to defects in the clearing of f-actin from the center of the blastodisc and f-actin fibrils do not reach a normal peripheral position (Fig. 5G; 10/11 with reduced clearing, compared to 1/15 in control-treated embryos). These effects on RNA segregation and f-actin rearrangements suggest a requirement for the microtubule network in the rearrangement of RNA-carrying f-actin bundles.
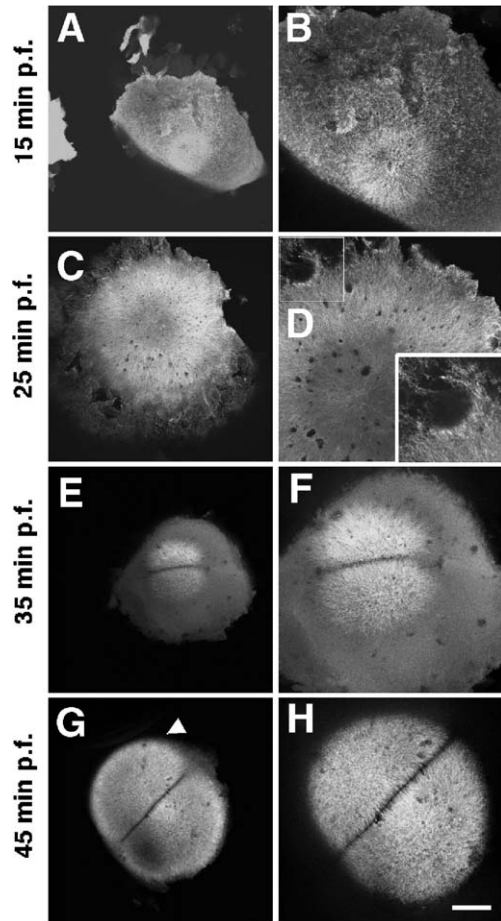
Fig. 4. Microtubule asters emanate from the center of the embryo during the early cellular cycles. Animal views of embryos fixed at progressively older stages of development (A, B: 15 min p.f.; C, D: 25 min. p.f.; E, F: 35 min p.f.; G, H: 45 min p.f.) and labeled with an anti-α-tubulin antibody. Left column: overview; right column, higher magnification views. The insert in panel D shows a higher magnification of the region labeled with a square. (A, B) Immediately after fertilization, a monoastral structure forms at the animal pole of the blastodisc. (C, D) Microtubules of this monoaster increase in length and reach the periphery of the blastodisc, which also exhibits local accumulations of shorter microtubules (inset). (E, F) Immediately prior to the first cleavage, a diastral structure flanking the prospective furrow. (G, H) As in the previous cycle, microtubules of this diaster increase to occupy more peripheral regions of the blastodisc. Scale bar in panel (H) represents 200 μm (left column) and 100 μm (right column).

If microtubule function is important for the reorganization of RNA-carrying f-actin, then interfering with proper microtubule dynamics by treatment of embryos with the microtubule-stabilizing drug paclitaxel (taxol) might also result in abnormal rearrangements. Paclitaxel treatment induces the formation of more prominent microtubule-based structures, such as the furrow microtubule arrays, which tend to remain in the embryo past stages in which they are normally disassembled (data not shown). These observations are consistent with this drug having a stabilizing effect on microtubules. FISH analysis shows that paclitaxel treatment results in an increase in aggregation of RNA particles at the periphery of the embryo. This effect can be most clearly visualized by the presence of midsize aggregates in regions of the RNA-rich domain that do not form part of the

internal boundary (Fig. 5D; 9/14 with increased peripheral aggregation, as defined by the presence of mid-size aggregates at least half-way into the region containing RNA aggregates, compared to 2/11 in control embryos). Similarly, a majority of embryos treated with paclitaxel show an increase in the degree of f-actin bundling at the periphery of the blastodisc (Fig. 5H; 4/7 with at least four peripheral bundles, compared to 0/15 in control embryos). These observations strengthen the idea that microtubules are involved in the movement towards the periphery and circumferential alignment of RNA aggregate-bound f-actin.

Interestingly, even though paclitaxel treatment does not interfere with the normal initiation of furrow formation (data not shown), very little or no RNA is recruited to the furrow in paclitaxel-treated embryos, and the majority of the RNA remains at the periphery of the blastomeres (Fig. 5D and data not shown). At later stages, the RNA accumulates into many large aggregates around the periphery of paclitaxel-treated embryo (data not shown). This observation suggests that proper microtubule destabilization, possibly once the RNAs have undergone partial aggregation, is important to allow the lateral movement of RNA aggregates towards the furrow and the recruitment of germ plasm in this location.

Cortical movement of dazl RNA-containing aggregates towards the animal pole and forming furrow

Time course analysis revealed that aggregates containing *dazl* RNA do not appear at the cortical surface of the blastodisc until 45 min p.f., which is approximately the time that the furrow is maturing and when the early animal RNAs have already initiated their recruitment at the furrow (Fig. 1). This is consistent with the observation that *dazl* RNA is translocated from the vegetal pole to the animal region during the early cleavage stages (Maegawa et al., 1999). Maegawa et al. observed the presence of *dazl* RNA in axial streamers, presumably as they are transported to the forming blastodisc from the vegetal cortex, which our studies corroborate (data not shown). Our FISH analysis, however, also reveals the presence of *dazl* RNA-containing aggregates at the egg cortex in progressively more animal regions as the cell cycle proceeds (Fig. 6). In freshly laid eggs, *dazl* RNA-containing aggregates are restricted to a region encompassing an approximately 30° arc centered on the vegetal most region of the egg cortex (Figs. 6A, B). Upon egg activation, these aggregates can be observed in progressively more animal positions of the egg cortex. Although some aggregates are relatively large and appear to translocate rather quickly in one region of the cortex (arrowheads in Figs. 6E, F), most of the aggregates are smaller and appear to translocate animally along the entire cortex (Figs. 6G, H). Our analysis indicates that a significant fraction of the *dazl* RNA moves animally via the cortex, and that its recruitment at the furrow coincides with the arrival of cortically bound aggregates to the animal region. These observations suggest that a primary pathway for the recruitment of *dazl* RNA is via animally directed translocation along the cortex (see Discussion).
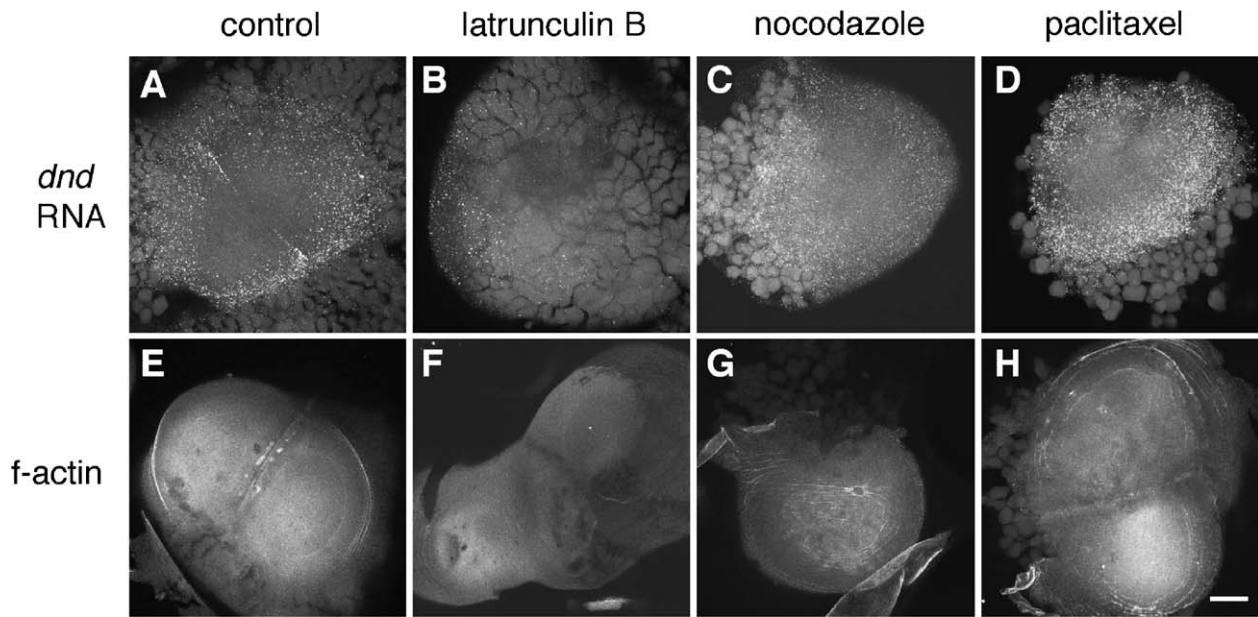
Fig. 5. Interference with cytoskeletal networks affects RNA aggregates and f-actin. Animal views of embryos at 45 min p.f. after treatment with control solvent (DMSO; A, E), injection of the f-actin inhibitor latrunculin B (B, F), and treatments with the microtubule-inhibiting reagent nocodazole (C, G) and the microtubule-stabilizing drug paclitaxel (D, H), and subsequently labeled for *dnd* RNA (A–D) or f-actin (E–H). Latrunculin-B-injected embryos show a reduction in the number of cortical RNA aggregates (B; in this particular embryo the reduction in the number of cortical aggregates is more pronounced on the right side of the embryo, presumably due to the uneven distribution of the injected drug), as well as defects in the formation of f-actin-based structures (F; 11/15 with defects in latrunculin-B-injected embryos, compared to 1/10 in control-injected embryos). Nocodazole-treated embryos show a reduction in the RNA-free zone at the center of the blastodisc and a decrease in the formation of larger RNA aggregates normally observable at this stage (C), as well as a reduction in the degree of clearing of f-actin from the center of the blastodisc (G). Paclitaxel-treated embryos show a general increase in RNA aggregation, which is observed in more peripheral locations than normal (D) and show increased degree of actin bundling at the periphery of the blastodisc (H). Scale bar in panel (H) represents 100 μm for all panels.

Separate RNA segregation pathways lead to a compartmentalized structure of the germ plasm

The separate modes by which different RNAs are segregated during early development suggest that there might be differences in their spatial localization within the germ plasm as it is recruited to the forming furrow. We therefore carried out double RNA in situ hybridization experiments to simultaneously label two RNAs in 4-cell stage embryos. In all experiments described below, control experiments showed that differences in localization pattern were not dependent on either the type of hapten or fluorescent substrate used for the double hybridization (data not shown). As expected from their localization at the furrow, the expression patterns of *vas*, *dnd*, *nos1*, and *dazl* RNAs all overlap to some degree within the furrow germ plasm aggregate. However, the extent of overlap between different RNAs varies, and this variation correlates with the segregation pathway for the RNAs. Double hybridization analysis shows that *vas* and *dnd* RNA localization patterns are essentially identical, apparently overlapping over the entire length of the main RNA-containing aggregates (Figs. 7A–D). Similarly, double labeling to detect *vas* and *nos1* RNAs reveals that *nos1* RNA localization also largely overlaps with that of *vas* RNA (Figs. 7E–H). However, in this case, we detect a slight but reproducible enrichment of *nos1* RNA in more medial regions of the furrow. Similar observations were obtained after colabeling of *dnd* and *nos1* RNAs (data not shown). Although we do not fully understand the basis for the slight medial

enrichment of *nos1* RNA, it is possible that it may be caused by the presence of a larger pool of *nos1* RNA in the blastodisc, which is suggested by in situ hybridization analysis (data not shown). In spite of the slight difference in *nos1* RNA enrichment, our observations show that the localization patterns of the early animal RNAs *dnd*, *nos1*, and *vas* are largely overlapping, which is consistent with their similar mechanism of segregation within the blastodisc.

On the other hand, double labeling of pairs involving any of the three early animal RNAs and *dazl* RNA shows a large degree of non-overlap between localization domains. Double labeling for either *vas* and *dazl* RNAs or *nos1* and *dazl* RNAs both shows that aggregates show a medial region enriched in early animal RNAs, an intermediate region containing both types of RNAs and a distal region enriched in *dazl* RNA (shown for *vas* and *dazl* in Figs. 7I–L). Thus, there is a correlation between the type of RNA segregation pathway and its site of enrichment at the furrow: after recruitment at the furrow, RNAs initially present at the animal pole occupy more medial positions along the furrow, while *dazl* RNA, which translocates from the vegetal pole along the egg cortex, occupies a more distal position.

It could be possible that early spatial differences in the recruitment of RNAs at the furrow would be transient and would disappear as the aggregating germ plasm matures. Alternatively, spatial differences may persist at later stages, which would suggest that the compartmentalized structure has a functional significance. In order to test these possibilities, we
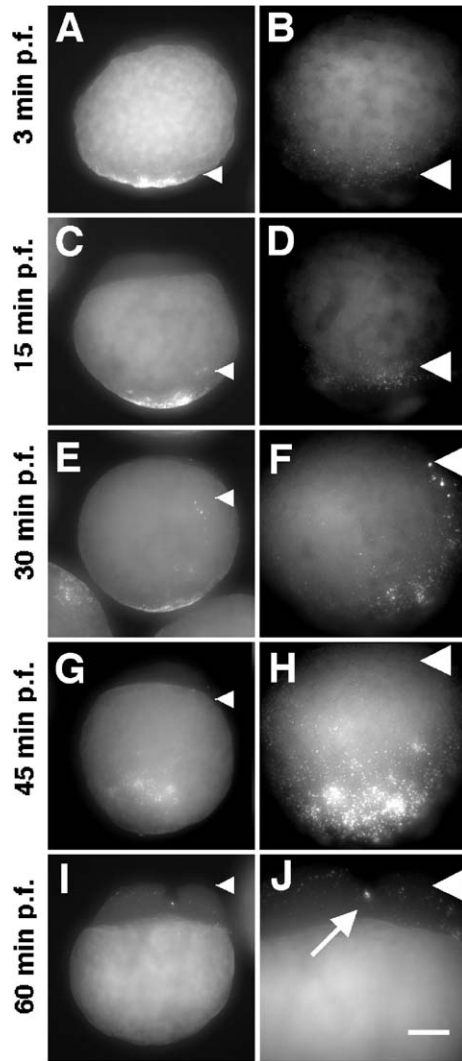
Fig. 6. Aggregates containing *dazl* RNA translocate towards the animal pole along the cortex during the first cell cycle. Animal views of embryos fixed at progressively older stages of development (A, B: 3 min p.f.; C, D: 15 min. p.f.; E, F: 30 min p.f.; G, H: 45 min p.f.; I, J: 60 min p.f.) and labeled with FISH to detect *dazl* RNA. All images are side views: left column: overviews; right column, higher magnification views of the cortex of embryos shown in the left panels. RNA aggregates can be observed at the vegetal pole in the freshly laid egg (A, B) and in progressively more animal positions along the cortex (in all panels, arrowheads indicate the animal most limit of the cortical region containing RNA aggregates). Recruitment of *dazl* RNA at the furrow (arrow in J) coincides with the appearance of cortical aggregates in animal regions. Scale bar in panel J represents 200 μm (left column) and 100 μm (right column).

colabeled *nos1* and *dazl* RNAs in embryos during the cleavage stages, at the 16-, 32- and 64-cell stages. Remarkably, the germ plasm aggregates, which by these stages have ingressed into single blastomeres, maintain a compartmentalized structure with respect to these two RNAs (shown at the 32-cell stage in Figs. 7M–P). In many aggregates, in the intermediate region where both types of RNAs overlap, the *dazl* RNA appears to surround the periphery of the *nos1* RNA-containing region (data not shown). During these stages, the *dazl* RNA-enriched region of the aggregate tends to maintain its original relation with the periphery of the embryo, remaining closest to this region. Thus, the compartmentalization of the germ plasm initiated during its

recruitment at the furrow is maintained during the early cleavage divisions, which is consistent with a functional role for the germ plasm substructure in the early embryo.

Discussion

Previous reports have shown that *vas*, *dnd*, *nos1*, and *dazl* maternal RNAs are all components of the zebrafish germ plasm, which aggregates at the furrow of the first and second cleavage planes. In this study, we have examined in detail these early patterns of localization and segregation and have addressed the role of cytoskeletal networks in these processes. We find that the RNAs exhibit separate pathways of segregation, and that these different pathways lead to a characteristic substructure of the germ plasm. We discuss these findings below and summarize them in Fig. 8.

Recruitment of early animal RNAs to the germ plasm: reliance on a microtubule-dependent rearrangement of the f-actin network

Three RNAs, *dnd*, *nos1*, and *vas*, which we refer to as the early animal RNAs, are present in small cortical aggregates that are enriched in a broad ring that encircles the animal pole of the egg. The relative absence of RNA aggregates in the center of this domain seems to be established during oogenesis, as it is present prior to the cytoskeletal rearrangements responsible for the movement towards the periphery of the aggregates during the first cell cycle (see below). Previous studies have shown that the animal pole cytoplasm is a wedge-like region of the oocyte established during oogenesis that can be distinguished by the presence of the oocyte nucleus, the sperm site of entry, the relative absence of yolk granules, and an enrichment in certain RNAs (reviewed in Pelegri, 2003). The enrichment of RNA cortical aggregates as a broad ring in this region suggests that the cortex at the animal pole itself has central and peripheral domains. Such a regional substructure in the cortex is perhaps not surprising since the presence of the sperm site of entry, a specialized actin-based structure at the center of the animal pole (Hart and Donovan, 1983; Hart et al., 1992), would be expected to confer different properties to the actin cortex. Further work analyzing the distribution of these RNA aggregates during oogenesis and egg activation will be required to determine the development of this ring-like prepattern of RNA localization at the animal cortex.

We show that aggregates containing early animal RNAs appear to be bound to an underlying filamentous network. During the first cell cycle, the domain containing these aggregates undergoes two main changes: first, the internal boundary of the domain (as seen on an animal view) appears to move outward, leaving a larger region in the center of the embryo that is free of RNA aggregates, and second, the aggregates appear to align along concentric rings centered around the animal pole. As these processes occur, aggregates appear to join with one another, growing in size to form medium-sized aggregates, and large aggregates of germ plasm form at the furrows.
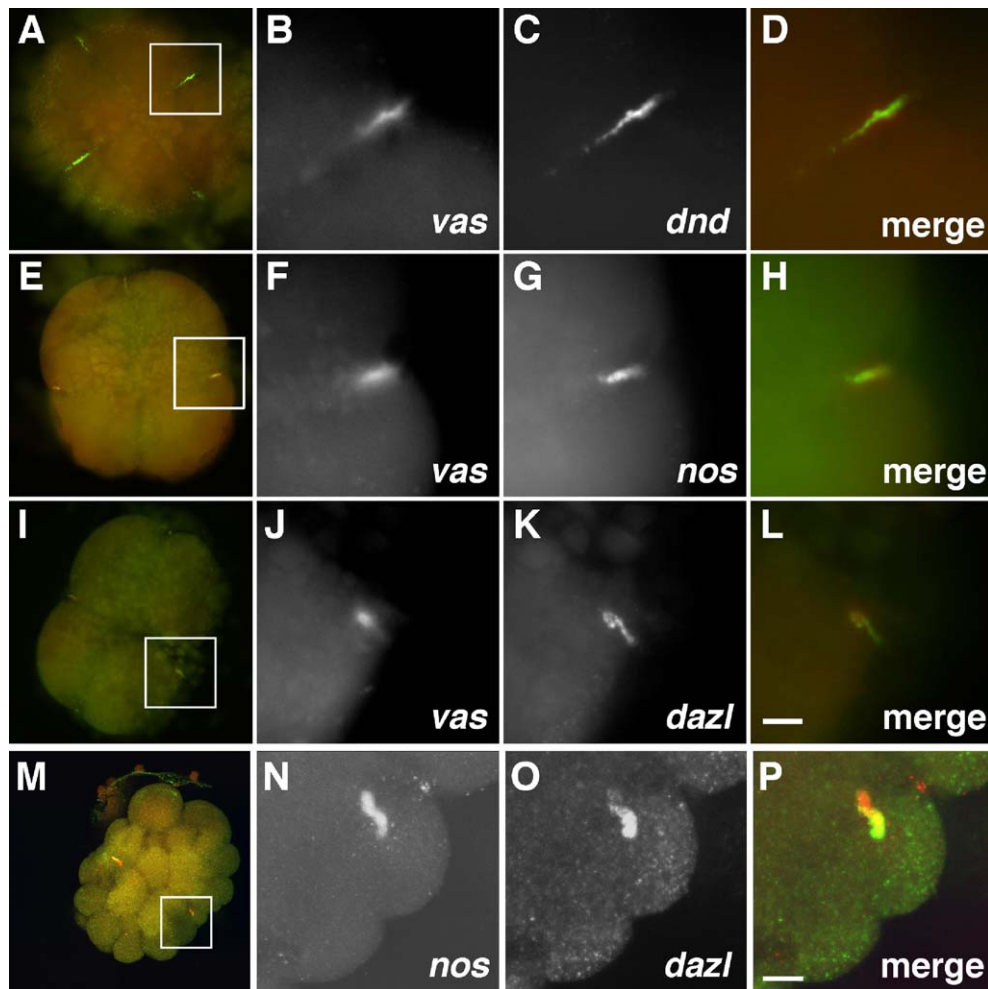
Fig. 7. Germ plasm RNAs are differentially enriched in different regions of the germ plasm. Animal views of embryos fixed at the 4-cell stage (A–L: 60 min p.f.) and the 32-cell stage (M–P: 1.75 hr p.f.) and labeled with FISH to detect different RNA pairs (A–D: *vas*, *dnd*; F–H: *vas*, *nos1*; I–J: *vas*, *dazl*; M–P: *nos1*, *dazl*). Left column: overview of merged images, right three columns: higher magnifications of the squared region in the left panels (middle two columns, in the same order as above; rightmost column, merged image with signals corresponding to the second and third columns in red and green, respectively). (A–H) During recruitment at the furrow of the 2- to 4-cells stage embryo, RNAs for *dnd*, *nos1*, and *vas* largely overlap (a slight enrichment in medial regions can be often observed for the *nos1* RNA (F–H)). Localization of these three RNAs shows a substantial region of non-overlap with the localization of the *dazl* RNA (I–L). At the 32-cell stage, the differential enrichment of *nos1* and *dazl* RNAs is maintained (M–P), showing that the germ plasm remains compartmentalized during the early cleavage stages. (A–L) Scale bar in panel L represents 100 μm (left column) and 25 μm (other three columns); (M–P) scale bar in panel P represents 120 μm (M) and 20 μm (N–P).

Our results indicate that the filamentous structure that is bound to the RNA aggregates likely corresponds to a network of f-actin bundles. A number of observations, from this study and previous reports, support this hypothesis: (a) ultrastructural analysis has shown that the *vas* RNA is associated with the actin cortex (Knaut et al., 2000); (b) f-actin forms a filamentous network of similar appearance to the filamentous network to which RNA aggregates appear to be bound; (c) the RNA-bound network and the f-actin network undergo similar movement towards the periphery as well as circumferential alignment during development; (d) RNA localization is reduced in embryos where the f-actin network is compromised after injection with the f-actin inhibitor Latrunculin B; and (e) the movement and realignment of the RNA-bound and f-actin networks exhibit a similar dependence on microtubule function, as shown by their behavior after treatment with microtubule-inhibiting and -stabilizing drugs (see below). In addition, both f-

actin and early germ plasm RNAs become recruited to the forming furrow, suggesting that common mechanisms may exist for their segregation during the first cell cycle. Unfortunately, current protocols to simultaneously label RNA aggregates and f-actin in fixed samples are incompatible, and thus, we have been unable to directly visualize this association. It therefore remains a formal possibility that the RNA aggregates interact with a second filamentous network whose arrangement depends on that of the f-actin network. The development of tools for imaging of RNA and f-actin in live zebrafish embryos will allow the direct examination of their association during development.

Our observations suggest that the movement towards the periphery and concentric alignment of the actin network and RNA aggregates depends on microtubule function. Inhibition of microtubule function with nocodazole results in a reduction in the central clearing of f-actin bundles and RNA aggregates. Conversely, exposure to the microtubule-stabilizing drug

paclitaxel results an increase in the peripheral accumulation of both f-actin and RNA aggregates. Consistent with this hypothesis, we have found that microtubules are present at the right time and place to exert an effect on the actin network. A monoastral structure emanating from a DNA structure, which is likely the male pronucleus, appears shortly after fertilization and grows in length until just prior to the initiation of the first cleavage cycle. This early monoaster is subsequently replaced by a diastral structure that appears during the initiation of the first mitotic cycle. Astral microtubules have been shown to attach to actin bundles at their distal ends and mediate their movement away from the center of the spindle both in intact cells (Waterman-Storer et al., 2000; Foe et al., 2000) and cell free lysates (Sider et al., 1999). Thus, it is possible that interactions between astral microtubules and f-actin mediate the movement towards the periphery of the latter, in turn leading to the movement of RNA aggregates. As the f-actin rearrangement occurs throughout egg activation and the first cell cycle, it is likely that both the early monoaster and the later appearing diaster are involved in this process.

Our observations suggest a model for the relationship between cytoskeletal rearrangements and germ plasm recruitment at the furrow (Fig. 8A). Small-sized RNA aggregates are bound to a cortical f-actin network in a prepattern at the animal pole that may depend on local differences at the animal cortex of the oocyte (Fig. 8A, left). The coordinated extension of astral microtubules may lead to the movement of f-actin cables towards the periphery and may promote their circumferential alignment (Fig. 8A, right). As this process occurs, actin bundling factors or motor proteins may facilitate increased contact between filaments and therefore further alignment as well as bundling into thicker cables. Circumferentially aligned f-actin would be expected to provide a favorable substrate on which RNA-containing particles can come into close proximity and coalesce into medium-size aggregates.

Subsequent recruitment into a single, rod-shaped large aggregate at each of the furrow ends appears to require the local, laterally directed movement of medium-size aggregates during furrow formation (blue arrows in Fig. 8A, bottom right). Although we do not yet understand the mechanistic basis for
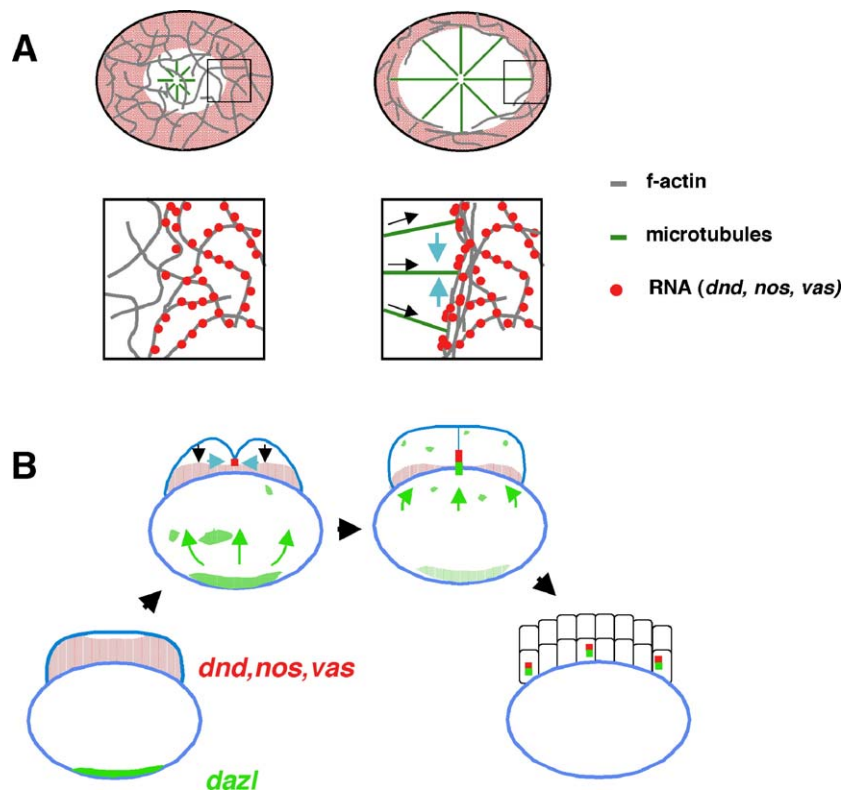

Fig. 8. Models for the recruitment of germ plasm RNAs at the furrow. (A) Cytoskeletal rearrangements and processes involved in the recruitment of early animal germ plasm RNA at the furrow. Diagrams show overview (top) and high magnification (bottom) views of embryos immediately after fertilization (left) and immediately prior to furrow formation (right). Embryos are drawn as animal views. RNA aggregates containing *dnd*, *nos1*, and *vas* RNAs are bound to a network of initially randomly oriented f-actin, forming a prepattern such that the central most region of the blastodisc is RNA-free. As development proceeds, the coordinated growth of astral microtubules (black arrows in bottom right inset) leads to the movement towards the periphery and circumferential alignment of f-actin. Aligned f-actin facilitates aggregation of RNA-containing particles. In a process whose mechanistic basis has not yet been addressed, lateral movement of aggregates in regions immediately adjacent to the forming furrow (blue arrows in bottom right inset) leads to the recruitment of aggregates at the furrow (not shown). (B) Relation of separate pathways of RNA segregation and the compartmentalization of the germ plasm. Embryos are drawn as side views, representing, from bottom left clockwise, a freshly laid egg, an embryo at an early stage of cellularization, an embryo at a late stage of cellularization, and an early blastula embryo. Early animal RNAs such as *dnd*, *nos1*, and *vas* (represented by red dots in stippled region), present in the animal cortex of the freshly laid egg undergo aggregation by the cytoskeletal rearrangements shown in (A) (black arrows) and recruitment at the furrow (large red aggregates) by proposed local lateral transport (blue arrows—see (A)). Vegetally localized RNAs such as *dazl* and presumably *bruno-like* reach the distal end of the forming aggregate at the furrow by translocation through the cortex (green arrows). These two mechanisms lead to a compartmentalized structure of the germ plasm, which is maintained during the early cleavage stages.

this process, the existence of local laterally directed transport which mediates recruitment is suggested by two observations. First, the limits of the recruited germ plasm aggregate along the forming furrow coincide with the limits of the band-like RNA-rich region that surrounds the furrow. Secondly, recruitment of RNA aggregates to the furrows coincides with the their disappearance in regions immediately adjacent to the furrow. We are currently investigating the factors involved in this laterally oriented movement of germ plasm aggregates towards the forming furrow.

Of interest, the stabilization of microtubule dynamics with paclitaxel increases aggregation at the periphery but interferes with its recruitment at the forming furrow. This may reflect a requirement for the dissociation of the microtubule network for the lateral movement of RNA aggregates towards the forming furrow. The observation of an enrichment of microtubules at the peripheral edges of the blastodisc is consistent with a role for microtubules in a process involving RNA aggregation or transient anchoring that is separate from their role in the movement of the f-actin network towards the periphery.

In summary, our analysis suggests a dynamic process in which f-actin-bound early germ plasm RNAs, such as *dnd*, *nos1*, and *vas*, translocate towards the periphery of the blastodisc via the microtubule-dependent movement of f-actin towards the periphery. This process in turn allows the aggregation of RNA-containing particles and their recruitment at the furrow. Other cytoskeletal rearrangements are likely involved in the further aggregation of the germ plasm already recruited at the furrow. Specifically, microtubules arrayed at the maturing furrow, which form the furrow microtubule array (FMA), appear to be inserted into the germ plasm aggregate and mediate the further aggregation and distal movement of the aggregate along the furrow (Pelegri et al., 1999).

Pathway of recruitment of vegetally localized germ plasm RNAs to the furrow

As opposed to the early animal germ plasm RNAs, which are initially present at the animal cortex of the egg, no *dazl* RNA cortical aggregates can be observed at the blastodisc until about 45 min p.f., approximately the same time when the first cleavage furrow begins to form. Previous reports indicated the presence of *dazl* RNA in axial streamers (Maegawa et al., 1999), the channels present in the yolk that serve during the first several cycles as the main route for ooplasmic streaming towards the forming blastodisc (Hisaoka and Firlit, 1960; Beams et al., 1985; Leung et al., 1998). We have also observed the presence of *dazl* RNA in axial streamers but find that there is also a cortical pathway for the animally directed movement of *dazl* RNA. Previous studies have shown the presence of a cortical microtubule network during the early cleavages that is important for the animally directed transport of a dorsalizing signal, which, like *dazl,* is thought to be anchored at the vegetal pole of the egg (Jesuthasan and Strähle, 1997). It is therefore possible that cortical transport of *dazl* RNA is similarly traveling along this same network of microtubules, a possibility that we are currently exploring. However, unlike the case of the

dorsal signal, which is thought to translocate solely along the prospective dorsal region of the embryo, *dazl* RNA aggregates appear to be moving along all regions of the cortex.

Two observations indicate that the cortical pathway of *dazl* RNA translocation may be involved in the transport of the *dazl* RNA that eventually is recruited at the furrow. First, upon fertilization, cortical aggregates containing *dazl* RNA can be observed in progressively more animal positions, and their movement along the cortex and arrival to the blastodisc roughly coincide with the appearance of *dazl* RNA at the site of germ plasm aggregation at the furrow. Secondly, the *dazl* RNA is recruited at the peripheral-most edge of the germ plasm, which is consistent with a scenario where cortical *dazl* RNA aggregates are trapped as they encounter the germ plasm aggregate at the furrow. It is unclear, however, whether *dazl* RNA that translocates along axial streamers provides a cytoplasmic pool that also contributes to the recruiting germ plasm. The resolution of this question will await the development of techniques that allow the visualization of *dazl* RNA as it segregates in live embryos.

Of interest, *dazl* RNA gradually accumulates in the cytoplasm of blastomeres during early cleavage (Maegawa et al., 1999; our own data), likely reflecting the gradual arrival of *dazl* RNA through axial streamers. In fact, in the mid-cleavage stages, the majority of *dazl* RNA in the blastomeres appears to be ubiquitously distributed. The presence of this large amount of *dazl* RNA, which is not part of the germ plasm, is insofar unexplained. However, two pathways for transport of *dazl* RNA could potentially contribute to separate pools of *dazl* RNA. It is possible that the cortical path constitutes a relatively rapid mechanism to transport RNA to the forming germ plasm, in time for its full assembly as the furrows form, while the axial path provides a less time-sensitive mode for the bulk of RNA to reach and accumulate at the blastodisc.

The RNA for the gene *bruno-like*, which has not been included in this study, has an initial vegetal localization similar to that of *dazl* and also aggregates at the distal ends of the furrow (Suzuki et al., 2000; Hashimoto et al., 2004). Therefore, we expect that this RNA may behave similar to *dazl* with respect to its late arrival at the cortex and the aggregating germ plasm. It remains to be determined whether *bruno-like* RNA, like *dazl* RNA, also utilizes both cortical and axial paths of transport and which of these pathways contributes to the aggregating germ plasm.

Compartmentalization of the zebrafish germ plasm

Our results show that two RNA segregation pathways, aggregation within the animal region and translocation from the vegetal cortex, lead to the recruitment of RNAs at the furrow during germ plasm aggregation (Fig. 8B). The early animal RNAs, for *dnd*, *nos1*, and *vas*, form a largely overlapping pattern that reflects their early presence in the animal pole and common segregation pathway. Strikingly, codetection of early animal RNAs and *dazl* RNA show a large degree of non-overlap. Thus, these localization patterns define compartments within the germ plasm with distinct RNA compositions along

the furrow: a medial domain enriched in the early animal RNAs *dnd*, *nos1*, and *vas*, an intermediate domain which contains both early animal RNAs and *dazl* RNA, and a distal domain enriched in *dazl* RNA. Moreover, the compartmentalization of the complex with respect to the early animal RNAs and *dazl* RNA is maintained during the early cleavage stages, which suggests a functional significance for this internal structure. Such a function could involve either the segregation of the germ plasm during the cleavage stages, such as the ingression from its peripheral location into discrete cells and its asymmetric segregation during cleavage (reviewed in Pelegri, 2003) or a role in the activation of germ plasm factors involved in the determination of primordial germ cells.

The differential enrichment of RNA at the germ plasm is reminiscent of the localization of RNAs at the *Xenopus* vegetal pole after transport via a region of the mitochondrial cloud (Kloc and Etkin, 1995). In this case, Xcat2, Xlsirts, and Xwnt11 RNAs are localized during early oogenesis in an overlapping layered patterned, with Xcat2 closest to the cortex and Xwnt11 farthest away from it. This similar behavior is also significant because Xcat2 is homologous to the *nos1* gene and segregates to the primordial germ cells (Mosquera et al., 1993; MacArthur et al., 1999). However, in the case of these *Xenopus* RNAs, this layered pattern is not clearly maintained at later stages of oogenesis (Kloc and Etkin, 1995). Our observations in the zebrafish provide to our knowledge the first example of a perduring compartmentalization of germ plasm components. Future studies will be aimed at understanding in detail the functional significance of the germ plasm structure, as well as potential links between its various compartments and other cellular components.

In summary, our results suggest a role for microtubule-dependent rearrangements of the f-actin network in the aggregation and recruitment at the furrow of germ plasm RNAs already present at the animal cortex, such as *dnd*, *nos1*, and *vas*. In addition, we show that vegetally localized RNAs such as *dazl* are recruited to the germ plasm at the animal pole at a later stage, likely after translocation along the egg cortex. RNAs that utilize these two pathways of recruitment become enriched in different regions within the zebrafish germ plasm, suggesting that separate segregation pathways may have evolved to facilitate the compartmentalization of this structure.

Materials and methods

Drug treatments

Nocodazole was prepared as a 5 mg/ml stock in DMSO and used at 1 μg/ml as in Pelegri et al., 1999. For the nocodazole treatment, embryos were collected approximately 5 min after they were laid and exposed to the drug diluted in embryonic medium (E3; Pelegri and Schulte-Merker, 1999). Paclitaxel was prepared as a 10 mM stock in DMSO and used at 10 μM in E3 medium. Paclitaxel treatments were carried out as the nocodazole treatments except that embryos were manually dechorionated following a brief exposure to Pronase and then treated with the drug. Latrunculin B was prepared as a 3 mg/ml stock in DMSO, diluted prior to use in water to 30 μg/ml, and injected into freshly laid eggs within 20 min after fertilization. Control embryos were treated or injected with a similar concentration of carrier solvent. Data for RNA aggregation are a

combination of results after FISH to detect *dnd* and *nos1* RNAs, which separately led to similar results.

Microtubule and f-actin labeling

For microtubule labeling, dechorionated embryos were fixed in 4% paraformaldehyde, 0.25% glutaraldehyde, 5 mM EGTA, and 0.2% Triton X-100 for 6 h at room temperature and overnight at 4°C. Fixed embryos were then washed in PBS, permeabilized in methanol overnight at −20°C, rehydrated in a methanol:PBS series, and treated with 0.5 mg/ml sodium borohydrate (30 min at room temperature, to inactivate remaining glutaraldehyde). Subsequently, and prior to labeling, the yolks of embryos were manually removed using forceps. After blocking in PBS with 0.1% Triton X-100 and 1% BSA for 1–4 h at room temperature, a monoclonal antibody against α-tubulin (Sigma monoclonal B5-1-2) at a 1:2500 dilution in PBS with 0.1% Triton X-100 was used to label microtubules overnight at 4°C. The primary antibody was recognized using an Alexa 488-conjugated rabbit anti-mouse antibody (Jackson ImmunoResearch) at a 1:100 dilution in PBS, 1% BSA, 0.1% Triton X-100. For labeling of f-actin, dechorionated embryos were fixed in 4% paraformaldehyde in PBS, manually deyolked, treated with 1% triton X-100 in PBS for 1 h to increase access to f-actin, and labeled with Alexa 488 phalloidin (Molecular Probes) for 20 min. Labeled embryos were also stained with DAPI (0.5 μg/ml in PBS) for 10 min at room temperature.

RNA in situ hybridization

Probes used have been previously described for *dnd* (Weidinger et al., 2003), *nos1* (Köprunner et al., 2001), *vas* (Yoon et al., 1997), and *dazl* (Maegawa et al., 1999). RNA in situ hybridization was performed as previously described (Pelegri and Maischein, 1998), except without the Proteinase K treatment. Detection of single probes with FISH was carried out with green fluorescent substrate, using an anti-hapten antibody conjugated to horseradish peroxidase and a substrate reaction with Alexa 488 tyramide solution (TSA Kit, Molecular probes, 1:100 dilution) in Amplification Buffer with 0.0015% hydrogen peroxide for 1 h at room temperature. For double fluorescent RNA in situ hybridization, one probe was digoxigenin labeled, and the other was fluorescein labeled. These probes were added simultaneously at concentrations of 1:100 in hybridization buffer and detected with anti-fluorescein alkaline phosphatase antibody (1:5000) and Fast Red substrate as previously described (Hauptmann and Gerster, 1994) and an anti-digoxigenin horseradish peroxidase antibody (1:1000) and Alexa 488 tyramide as above.

Imaging

Following detection, embryos were fixed with 4% paraformaldehyde for at least 2 h to fix the product of the substrate reaction and then transferred to 30% and then 50% glycerol:PBS for long-term storage at 4°C before mounting. For images in animal views, embryos labeled with fluorescent probes were deyolked after labeling, and the blastodiscs were mounted flat on a microslide. Fluorescent images were taken using either a Zeiss Axioplan2 fluorescent microscope and Open Lab imaging software or a BioRad confocal microscope. Unless otherwise specified, images are flat projections of z-stack optical sections spanning the width of the imaged embryo or subcellular structure.

References

Beams, H.W., Kessel, R.G., Shih, C.Y., Tung, H.N., 1985. Scanning electron microscopy studies on blastodisc formation in the zebrafish, *Brachydanio rerio*. J. Morphol. 184, 41–50.

Becker, K.A., Hart, N.H., 1999. Reorganization of filamentous actin and myosin-II in zebrafish eggs correlates temporally and spatially with cortical granule exocytosis. J. Cell Sci. 112, 97–110.

Braat, A.K., Zandbergen, T., van de Water, S., Goos, H.J.T., Zivkovic, D., 1999. Characterization of zebrafish primordial germ cells: morphology and early distribution of *vasa* RNA. Dev. Dyn. 216, 153–167.

Dekens, M.P.S., Pelegri, F.J., Maischein, H.-M., Nüsslein-Volhard, C., 2003. The maternal-effect gene futile cycle is essential for pronuclear congression and mitotic spindle assembly in the zebrafish zygote. Development 130, 3907–3916.

Foe, V.E., Field, C.M., Odell, G.M., 2000. Microtubules and mitotic cycle phase modulate spatiotemporal distributions of F-actin and myosin II in *Drosophila* syncytial blastoderm embryos. Development 127, 1767–1787.

Hart, N.H., Donovan, M., 1983. Fine structure of the chorion and site of sperm entry in the egg of *Brachydanio*. J. Exp. Zool. 227, 277–296.

Hart, N.H., Becker, K.A., Wolenski, J.S., 1992. The sperm site during fertilization of the zebrafish egg: localization of actin. Mol. Reprod. Dev. 32, 217–228.

Hashimoto, Y., Maegawa, S., Nagai, T., Yamaha, E., Suzuki, H., Yasuda, K., Inoue, K., 2004. Localized maternal factors are required for zebrafish germ cell formation. Dev. Biol. 268, 152–161.

Hauptmann, G., Gerster, T., 1994. Two-color whole-mount in situ hybridization to vertebrate and *Drosophila* embryos. TIG 10, 266.

Hisaoka, K.K., Firlit, C.F., 1960. Further studies on the embryonic development of the zebrafish, *Brachydanio rerio* (Hamilton-Buchanan). J. Morphol. 107, 205–225.

Howley, C., Ho, R.K., 2000. mRNA localization patterns in zebrafish oocytes. Mech. Dev. 92, 305–309.

Jesuthasan, S., 1998. Furrow-associated microtubule arrays are required for the cohesion of zebrafish blastomeres following cytokinesis. J. Cell Sci. 111, 3695–3703.

Jesuthasan, S., Strähle, U., 1997. Dynamic microtubules and specification of the zebrafish embryonic axis. Curr. Biol. 7, 31–42.

Kishimoto, Y., Koshida, S., Furutani-Seiki, M., Kondoh, H., 2004. Zebrafish maternal-effect mutations causing cytokinesis defects without affecting mitosis or equatorial *vasa* deposition. Mech. Dev. 121, 79–89.

Kloc, M., Etkin, L.D., 1995. Two distinct pathways for the localization of RNAs at the vegetal cortex in *Xenopus* oocytes. Development 121, 287–297.

Kloc, M., Etkin, L.D., 2005. RNA localization mechanisms in oocytes. J. Cell Sci. 118, 269–282.

Knaut, H., Pelegri, F., Bohmann, K., Schwarz, H., Nüsslein-Volhard, C., 2000. Zebrafish *vasa* RNA but not its protein is a component of the germ plasm and segregates asymmetrically prior to germ line specification. J. Cell Biol. 149, 875–888.

Köprunner, M., Thisse, C., Thisse, B., Raz, E., 2001. A zebrafish nanos-related gene is essential for the development of primordial germ cells. Genes Dev. 15, 2877–2885.

Leung, C.F., Webb, S.E., Miller, A.L., 1998. Calcium transients accompany ooplasmic segregation in zebrafish embryos. Dev. Growth Differ. 40, 313–326.

MacArthur, H., Bubunenko, M., Houston, D.W., King, M.L., 1999. Xcat2 is a translationally sequestered germ plasm component in *Xenopus*. Mech. Dev. 84, 75–88.

Maegawa, S., Yasuda, K., Inoue, K., 1999. Maternal mRNA localization of zebrafish DAZ-like gene. Mech. Dev. 81, 223–226.

Mosquera, L., Forristall, C., Zhou, Y., King, M.L., 1993. A mRNA localized to the vegetal cortex of *Xenopus* oocytes encodes a protein with a nanos-like zinc finger domain. Development 117, 377–386.

Pelegri, F., 2003. Maternal factors in zebrafish development. Dev. Dyn. 228, 535–554.

Pelegri, F., Maischein, H.-M., 1998. Function of zebrafish β-catenin and TCF-3 in dorsoventral patterning. Mech. Dev. 77, 63–74.

Pelegri, F., Schulte-Merker, S., 1999. A gynogenesis-based screen for maternal-effect genes in the zebrafish, *Danio rerio*. In: Detrich, W., Zon, L.I., Westerfield, M. (Eds.), Methods in Cell Biology, vol. 60. Academic Press, San Diego, pp. 1–20.

Pelegri, F., Knaut, H., Maischein, H.-M., Schulte-Merker, S., Nüsslein-Volhard, C., 1999. A mutation in the zebrafish maternal-effect gene nebel affects furrow formation and *vasa* RNA localization. Curr. Biol. 9, 1431–1440.

Sider, J.R., Mandato, C.A., Weber, K.L., Zandy, A.J., Beach, D., Finst, R.J., Skoble, J., Bement, W.M., 1999. Direct observation of microtubule-f-actin interaction in cell free lysates. J. Cell Sci. 112, 1947–1956.

Suzuki, H., Maegawa, S., Nishibu, T., Sugiyama, T., Yasuda, K., Inoue, K., 2000. Vegetal localization of the maternal mRNA encoding an EDEN-BP/ Bruno-like protein in zebrafish. Mech. Dev. 93, 205–209.

Waterman-Storer, C., Duey, D.Y., Weber, K.L., Keech, J., Cheney, R.E., Salmon, E.D., Bement, W.M., 2000. Microtubules remodel actomyosin networks in *Xenopus* egg extracts via two mechanisms of F-actin transport. J. Cell Biol. 150, 361–376.

Weidinger, G., Stebler, J., Slanchev, K., Dumstrei, K., Wise, C., Lovell-Badge, R., Thisse, C., Thisse, B., Raz, E., 2003. *dead end*, a novel vertebrate germ plasm component, is required for zebrafish primordial germ cell migration and survival. Curr. Biol. 13, 1429–1434.

Wylie, C., 1999. Germ cells. Cell 96, 165–174.

Yoon, C., Kawakami, K., Hopkins, N., 1997. Zebrafish *vasa* homologue RNA is localized to the cleavage planes of 2- and 4-cell-stage embryos and is expressed in the primordial germ cells. Development 124, 3157–3165.